

A study of power management approach in a grid connected hybrid renewable generation system

Pranita Rathod¹, Sujit Kumar Bhuyan², Sanjay Kumar Mishra¹

¹Department of Electrical Engineering, G. H. Raisoni University Amravati, Maharashtra, India

²Resource Assessment and Asset Analysis (RAAA) Manikaran Analytics Limited, New Delhi, India

Article Info

Article history:

Received Jul 16, 2022

Revised Jan 19, 2023

Accepted Feb 9, 2023

Keywords:

Auxiliary unit
Battery storage unit
Improved P&O
PV module
THD

ABSTRACT

Where sun irradiation is not continuous throughout the day, photovoltaic (PV) cells are used to supply solar power to the grid. A suitable power management plan is required to provide a steady power supply to the grid. The hybrid renewable generation system (HRGS) interconnected to the grid is the subject of this study, which provides a revolutionary power management method and control strategy. PV devices, a battery storage unit (BSU) charged by electricity generated from solar energy, and an auxiliary unit make up the HRGS concept (AU). Maximum power point tracking (MPPT) uses an improved perturb and observe (P&O) method to track maximal energy from solar irradiation. The peculiarity of this approach is that it uses a modified MPPT algorithm to handle power management throughout the process, allowing it to manage continuous power delivery to the grid based on load demand. It is capable of working under any load situation. The action of an L-C filter is utilized to decrease the total harmonic distortion (THD). The HRGS scheme's performance appraisals work correctly, achieve maximum productivity, and continually managing the power provided to the grid in a satisfactory way.

This is an open access article under the [CC BY-SA](https://creativecommons.org/licenses/by-sa/4.0/) license.



Corresponding Author:

Sujit Kumar Bhuyan

Resource Assessment and Asset Analysis (RAAA) Manikaran Analytics Limited

New Delhi, India

Email: sujeet.kumar84@gmail.com

NOMENCLATURE

EES	: Electrical energy storage	I_{MP}	: The current belongs to maximum amount power of the PV cell [V]
HPS	: Hybrid power system	I_{PV}/I_{ph}	: PV panel output current [A]
MPP	: Maximum power point	V_{oc}	: PV panel open-circuit voltage [V]
PCC	: Point of common coupling	I_{SC}	: Photovoltaic cell current Short-circuit [A]
pf	: Power factor	K_I	: Temperature coefficient related to ISC
PLL	: Phase lock loop	N_s	: Photovoltaic cell or module
PWM	: Pulse width modulation	R_s	: Series resistance [Ω]
RESs	: Renewable energy sources	R_{sh}/R_p	: Parallel resistance [Ω]
SCS	: Supervisory control scheme	V_{MP}	: The voltage belongs to maximum amount power of the PV module [A]
SOC	: State of charge	N_{par}	: Modules in parallel in a PV array
TD	: Tracking direction	K_V	: Temperature coefficient related to V_{oc}

THD	: Total harmonics destruction	P_{aux}	: Output power of Boost converter connected to AU
VSC	: Voltage source converter	P_b	: Battery output power [W]
VSCC	: Voltage source converter control	P_{batt}	: Buck-boost converter output power connected across BSU [W]
I_o	: Reverse threshold current [A]	P_{dc}	: DC bus power [W]
a	: Completion or ideality factor (= 1.3)	Q_m	: Maximum charge of battery [AH]
k	: Boltzmann's constant [= $1.3806503 \times 10^{-23} \text{ J}^\circ\text{K}$]	R_a	: Internal resistance [Ω]
V	: Terminal voltage of Photovoltaic panel [V]	R_b	: Terminal resistance [Ω]
G	: Irradiation on the device surface [$\frac{\text{W}}{\text{m}^2}$]	V_a, V_b, V_c	: Grid voltages
T	: Temperature of PV panel [K]	I_a, I_b, I_c	: Grid currents
d	: Control action	V_{aux}	: Auxiliary voltage [V]
q	: Electron charge [= $1.60217646 \times 10^{-19} \text{ C}$]	V_{batt}	: Battery voltage [V]
C_i	: Incipient Capacitance [F]	V_{dc}	: DC bus voltage [V]
C_p	: Polarization Capacitance [F]	V_{ocv}	: Open circuit voltage of BSU
I_{aux}	: Auxiliary Current [A]	L_1	: Constant load (priority load)
$I_{auxboost}$: Output current of Boost converter connected to AU [A]	L_2	: Fluctuating load (less-priority load)
I_{batt}/I_{tb}	: Battery current [A]	P_{L1}	: Constant load or priority load [W]
I_{dc}	: DC bus current [A]	P_{L2}	: Less priority or variable load [W]
P_{Load}	: Total load [W]		

1. INTRODUCTION

In recent years, HRGS have become more versatile and appealing, allowing them to satisfy load demand. It can be used as a stand-alone device or as part of a grid. Global warming is caused by traditional sources such as fossil fuels, thermal energy. As a result, it contributes to increased pollution and climate change around the planet. Furthermore, over the last two decades, electricity usage has skyrocketed. According to the survey, power usage would increase by roughly 56 percent to 60 percent between now and 2050 [1], [2]. The primary problems we face are reducing pollution and increasing electricity generation in order to compensate for rising energy demand by utilizing renewable energy sources. Increased environmental pollution as a result of increased carbon emissions into the atmosphere from the use of more fossil fuels [3], which poses a health risk to all living things and leads to an increase in global temperature and climate change. Conventional power generations' typical statements are constrained. It's possible that it'll be depleted in the following years. In such a situation of increased requirement of power generation and load demand, other alternative of power generation is essential. As a result, renewable energy generation is critical for increasing the strength needed to compensate for conventional power generation's deficiencies. It is vital to create more electricity in a reliable method due to improvements in cutting-edge virtual technologies and a comfortable life style.

The proposed scheme creates a strong desire to incorporate a HRGS that can send power to the grid or work in a standalone mode. When the HRGS system is attached to the grid, however, there may be a power management issue. Sometimes, it gives more power when there is a less demand and on the other way it gives less power at the time of more load demand. So, without maintaining proper power management, the HRGS unable to generate power without controlling the BSU and AU. To maintain proper power delivery throughout the complete day, an alternate control strategy of HRGS is required.

The HRGS system makes use of a modified P&O algorithm to maintain optimum power management. At any time when load demand is high, HRGS with an L-C filter design unit is used to lower the harmonic content of voltage and current signals connected to the grid. The HRGS control approach is demonstrated while preserving power management under various SOC conditions of the BSU. The proposed scheme's ultimate goal is to ensure a constant power supply by regulating the power stored in the BSU and applying AU power to the grid. The AU could be a diesel generator, fuel cell, or super capacitor that can generate or store energy when the grid needs it. HRGS' power management and control approach are properly managed, depending on the grid's load requirement, thanks to a suitable algorithm.

The THD value of the voltage and current signal of the HRGS system connected to the grid has also been kept below the threshold value (less than 5 percent). This is the unique grid-connected power management and control strategy system, which is also detailed in the simulation results section. The HRGS technique utilized here is both environmentally benign and cost-effective in ensuring grid continuity in the event of a load outage.

As we know that the renewable energy sources (RESs) are the clean sources of energy and found abundantly across the world. This HRGS scheme can be applied to any parts of the world. From all types of RESs, the solar power has been utilized since decades and promising alternative sources to meet the power demand growth. The main advantages of using this solar energy sources are available at an acceptable cost. It is estimated that around 11% of solar power generation has been utilized [4]. Therefore, there is a tremendous energy market growth using solar power generation. However, due to the weather condition (rainy, cloudy, less solar irradiation), solar energy alone cannot fulfil the energy demand. Therefore, an alternative hybrid energy system may be selected in order to fulfil the continuous demand of energy growth. The hybrid energy system may include various renewable energy system, sometimes it may not suitable to give continuous power supply to the grid (wind and solar) or sometimes it may provide more power generation to fulfil the market needs, but the extra surplus power must be stored using BSU and AU. The proper power management and maintaining continuous power supply to the grid is a very important aspect to understand. An alternative hybrid energy sources Wind, Solar and Tidal, battery, SC and FC are also integrated, but the complexity of power management aspect increases, which is difficult to control and better the performance of the system [5]–[7]. Some strategies are carried out to improve the implementation of PV system in residential as well as at utility scale. Among this payback period and cost reduction are the main significant issues of PV system utility holders. Reduced cost analysis and comparison to other renewable energy sources shows that the PV system performance is better with relation to life period. Innovation of technologies is further essential in these fields to enhance the performance of PV cell of HRGS system is described as follows: i) Components such as PV cells, batteries, switches and sensors are to be manufactured based on less cost and more life so as to have higher performance; ii) Advancement of power converter component leads to power maximization and less harmonic content to maintain the grid voltage and current waveforms; and iii) Using proper power managing scheme to improve the effectiveness of HRGS and its reliability.

Countless efforts are made to improve the effectiveness of PV model that are connected to the grid [8]–[12]. In [8] 3 ϕ grid connected to single stage PV model. In this system MPPT algorithm, enhance the effectiveness of grid connected PV model with rapid change of irradiation. Intelligent PV module [9] is implemented so as to reduce the system loss. In this system, PV array with intelligent PV modules using MPPT are reordered. In [11] optimal sizing of the PV module is suggested, proper use of PV sizing type and inclination of AC/DC converter. The advantages of using this scheme are to enhance the performance of grid connected PV module. Battery storage optimization capacity in PV/battery hybrid system has been discussed in [12]. Battery capacity can be enhanced concerning on net present value and self – sufficiency ratio. Some improvement of output accuracy is also discussed [13] but the system becomes more complex and costly due to the large number of active-clamp circuit, ZVT-interleaved DC/DC converter and accurate state model. Multilevel DC/DC converter and quasi-Z-source inverter QZSI are also employed in grid connected PV system [13], [14] to reduce the harmonic components in the waveform and operates at unit pf. Several power management strategies have been worked out on PV/battery systems. However, it is unable to address the performance of the system, accuracy for elimination of harmonics. Power management strategy is also employed in multiple PV/battery system, which has been discussed [15], [16] in which particular unit load condition is allotted to different units but unable to address the power management control strategy and its performance. PV/battery hybrid system is presented [17], in which SOC of storage unit and micro grid voltages are operated by distributed control framework. In this BSU is employed with PV array for water pumping system supervision. The paper [18] is discussed on supervision strategy, which is based on SOC monitoring of BSU. In photovoltaic/battery system, a decentralized control and newly architectural approach has been discussed to control the power management, where the battery storage is connected to DC bus [19]. In [20], [21] the power management strategy of a PV/battery system linked to the grid or islanded manages the active and reactive power and regulates the voltages of DC and AC buses. Furthermore, the system performance under battery overcharging and deep charging modes, as well as the power consumption and cost that can be optimized by the smart power management system, may be thoroughly investigated. [22]. the modified genetics algorithm (GA) is also used in this smart management system with or without the preference of user for the load allocation and multi-objective optimization, which is used for the micro grid organization [23]. The main aim of using power optimization is to reduce the cost function and discharge for supplying power to the grid. Thus, the continuity of supply is restored at any adverse situation. The decision about the sizing of generator according to the cost turn out to be more financial burden [24]. The optimization of HRGS has been suggested [25], [26]. PV in addition to BSU has been implemented in

residential and commercial building which is discussed [27], [28]. It is suggested that the different sizing and the analysis of different behavior of various combinational types of HRGS performs well to achieve higher accuracy of the system. PV with wind and BSU works as a back-up purpose, but it seems that it is not the perfect combination because PV as well as wind both are intermittent nature. The power generation is always varying in nature. Sometimes it may happen that solar radiation and wind speeds are not up to the mark for sufficient power generation. This system sometimes works as sluggish and will not be a more economical choice as compared to power management and continuity of power supply. Thus, the strong motivation behind this using the scheme is to model an alternative hybrid renewable generation system (HRGS) and implement an algorithm to manage the power and its control strategy to achieve higher performance and continuity of power supply and harmonic reduction as per the need of load at any unfavorable condition based on priority and less priority nonlinear load. In our HRGS system the analysis of proper power management strategy, control of power management and battery storage and auxiliary unit has also been discussed in the subsequent section. Further, as per the performance is concerned, harmonic reduction and THD calculation of voltage and current signal analysis has also been carried out before or after supplying the grid. This scheme is more economical, higher performance and accuracy compared to the existing analysis discussed in the above-mentioned literatures.

The suggested HRGS model contain three components: PV, BSU, and AU. New power management and control approach has been designed for managing the power flow between the photovoltaic, BSU, and AU in line with the grid's load demand. Both higher and lower priority loads are factored into the grid load demand. The control approach proposed for maintaining the reliability of the HRGS system's power supply has been thoroughly presented in the simulation results section. The HRGS model is attached to the grid by VSCC. After synchronization, the grid voltage is properly matched with the HRGS voltage. An improved P&O algorithm is employed in the photovoltaic system to obtain maximal power. After attaining maximum power, the surplus electricity is stored in the BSU and then distributed to the microgrid. On the other hand, grid demand changes based on load demand. A power management strategy is required in this instance to meet the grid's adequate power requirements. Load shedding is an option if there is a disparity between the load required and the HRGS system's power generation. How will we ensure that the system receives adequate electricity without resorting to load shedding? The findings section goes into great detail on this. The harmonic reduction section is then examined in order to increase the power quality of the voltage and current signals. The harmonic content of a signal connected to the grid under any load state is determined via THD analysis of voltage and current signals. The HRGS model is now connect to the microgrid for the first time. The outline of the paper is divided into sections. Section 2 digs into the modelling of the proposed HRGS system as well as the elements of the PV system, in addition to section 1, which deals with the introduction to the proposed study. Section 3 looks at several types of control techniques for various systems, while Section IV goes through the HRGS simulation findings and analysis.

2. GRID-CONNECTED HRGS MODELLING

Figure 1 shows the suggested HRGS model coupled to a three-phase grid. PV/BSU/AU are the components. The entire system is powered by a three-phase AC load. The 3ϕ AC load may be a priority type load or a reduced priority type load depending on the load demand. In this case, a higher priority load denotes a non-linear or constant load, while a lower priority load denotes a variable load. The PV system uses MPPT to track maximum power and supplies it to a DC/DC converter. PV's output voltage has been raised with the help of a boost converter. Energy is stored in the primary storage unit (BSU) and delivered to the grid as needed. BSU supplies the load for a long time when PV power generation is unavailable, but it is unable to supply the power demand on its own. A bi-directional DC/DC converter is located across the BSU (buck-boost converter). The purpose is to charge and discharge the BSU, with power stored in the BSU and distributed to the grid as needed. When both the PV and the BSU are not able to provide power to the load, an AU is used as a backup. The AU can also be used to store energy in the BSU until it reaches its maximum capacity (SOC level). These sources, which are connected in parallel, supply all three-phase local loads. An LC filter is developed and coupled across the HRGS to minimize harmonics and improve the power quality of voltage and current signals. The THD calculation was finished, and the outcome was within the tolerance limit (less than 5 percent) The HRGS system is depicted in Figure 1.

2.1. Photovoltaic (PV) model

PV is a semiconductor device consisting of p-n junction diode. The equivalent PV cell circuit diagram is depicted in Figure 2. The mathematical model of a PV module has been referred from [28]. The MPPT algorithm is utilized to suggest the highest amount of power from a PV system using improved P&O method [29]. The equations from the article [28]-[30] were used to plot the PV system. Table 1 summarizes

the PV array specifications. In the proposed hybrid renewable energy system, the Sun Power SRP-305-WHT solar panel is planned and projected using MATLAB 2019 SIMULINK.

$$I = I_{PV} - I_0 \left[\exp\left(\frac{V+R_S I}{V_t a}\right) - 1 \right] - \frac{V+I R_S}{R_P} \tag{1}$$

Where $V_t = \frac{k T N_S}{q}$

$$I_{PV} = (I_{PVn} + K_I \Delta_T) \frac{G}{G_n} \tag{2}$$

Where $\Delta_T = T - T_n$ and $I_{PVn} = \frac{R_p + R_s}{R_p} I_{SCn}$

$$I_0 = \frac{I_{SCn} + K_I \Delta_T}{\exp\left(\frac{V_{OC} + K_V \Delta_T}{a V_t}\right) - 1} \tag{3}$$

$$I = I_{PV} N_{par} - I_0 N_{par} \left[\exp\left(\frac{V+R_S \left(\frac{N_{ser}}{N_{par}}\right) I}{V_t a N_{ser}}\right) - 1 \right] - \frac{V+R_S \left(\frac{N_{ser}}{N_{par}}\right) I}{R_P \left(\frac{N_{ser}}{N_{par}}\right)} \tag{4}$$

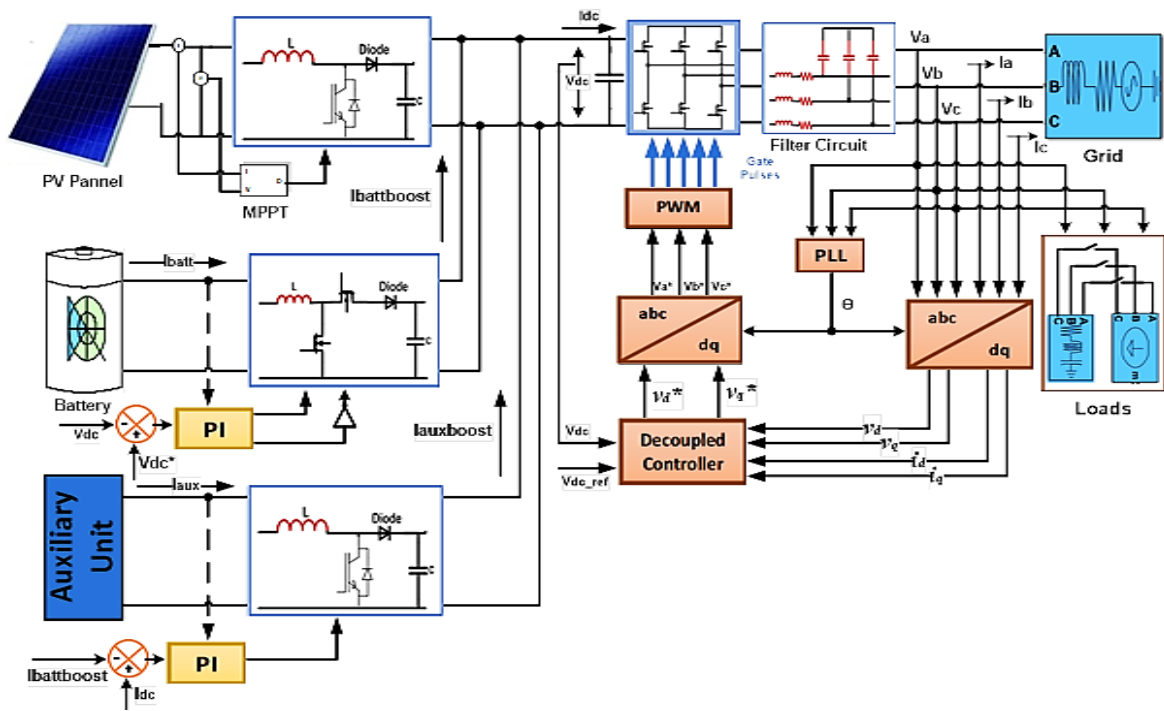


Figure 1. HRGS Simulink model linked to the grid

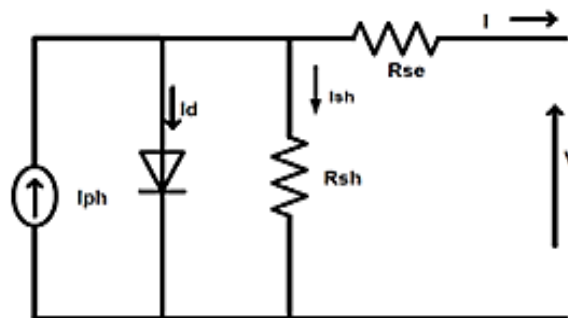


Figure 2. PV Array model with a single diode

Specification	Value
N_{par}	66
N_{ser}	05
I_{MP}	5.58 A
Irradiance	1000
I_{SC}	5.96 A
K_I	3.5 mA/°C
K_V	-176.6 mV/°C
Maximum power of the PV panel (Pmax)	305 W
N_s	96
Temperature (T)	25
V_{MP}	54.7 V
V_{OC}	64.2 V

2.2. Improved P&O with MPPT

The standard P&O approach is useless for keeping the changeable solar radiation since it varies consistently about the MPP when the peak power of the photovoltaic system is fixed at a specific functional point and deviates from MPP during variations in solar radiation. The bifurcation is caused by variable degrees of irradiation. PV module energy losses arise as a result of this. The classic P&O technique has been addressed [31]–[35]. A improved P&O method was devised to address these limits. The voltage and current are calculate first, and then the power is determined. The work flow of improved P&O method is depicted in Figure 3. The performance of improved P&O is enhanced by modifying the current (ΔI) parameter. The modified P&O algorithm has a range of control actions, as shown in Table 2. There are eight scenarios to think about. The power differential (ΔP) determines the tracking direction and control results. Examining two different types of test cases demonstrates this. Test Case-1: If the changes in voltage (V) and current (I) have opposing signs, the PV module is in continuous irradiation. Test Case-2: The PV module is irradiated differently if the changes in V and I have the same sign.

Under steady radiation, the suggested MPPT approach performed comparable to standard P&O. When the radiation fluctuates, however, this MPPT technique performs differently than the traditional P&O approach. For speed tracking, the step size is increased to twice throughout the insufficient tracking period. As a final result, the updated P&O algorithm may smooth out power fluctuations caused by solar irradiation or reference voltage fluctuations. As a result, MPP divergence, as per to the article [36].

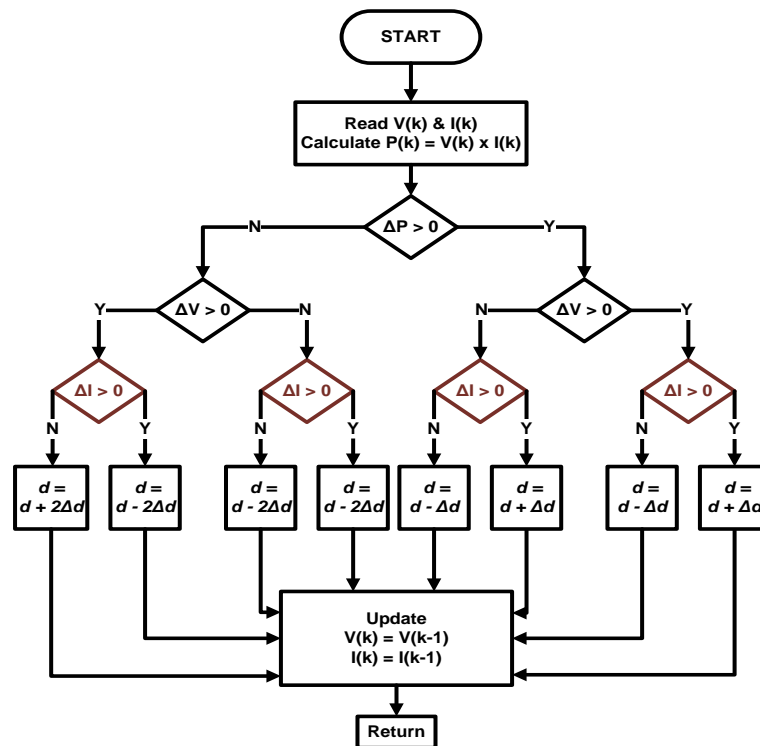


Figure 3. Work flow of modified P&O algorithm

Table 2. Modified P&O algorithm has several control actions

Case	ΔV	ΔP	ΔI	G	TD	d
1	'+'	'+'	'+'	Increase	True	'd' = 'd + Δd '
2	'+'	'+'	'-'	Constant	True	'd' = 'd - Δd '
3	'+'	'-'	'+'	Increase	Wrong	'd' = 'd - 2 Δd '
4	'+'	'-'	'-'	Constant	Wrong	'd' = 'd + 2 Δd '
5	'-'	'+'	'+'	Constant	True	'd' = 'd + Δd '
6	'-'	'+'	'-'	Decrease	True	'd' = 'd - Δd '
7	'-'	'-'	'+'	Constant	Wrong	'd' = 'd - 2 Δd '
8	'-'	'-'	'-'	Decrease	Wrong	'd' = 'd - 2 Δd '

2.3. Battery storage unit (BSU) model

Figure 4 depicted the mathematical model of BSU. The SOC, the voltages of a and b phase e_a , e_b are the state variables. The (5) to (9) has been alluded from [37]. The parameters for the BSU are listed in Table 3. The Lithium-ion battery model's specifications are listed in Table 3. The circuit diagram of the improved P&O approach as depicted in Figure 4.

$$V_{ocv} = 338.8 \times [0.94246 + 0.05754 \times SOC] \tag{5}$$

$$R_a \cdot C_p \cdot \frac{de_a}{dt} + \left(\frac{R_a + R_b}{R_b}\right) \cdot e_a = V_{oc} + \frac{R_a}{R_b} \cdot e_b \tag{6}$$

$$R_b \cdot C_i \cdot \frac{de_b}{dt} + e_b = e_a - R_b \cdot I_{tb} \tag{7}$$

$$\frac{dSOC}{dt} = \frac{I_{tb}}{Q_m} \tag{8}$$

$$I_{tb} = \frac{[V_{oc} - \sqrt{V_{oc}^2 - 4(R_a + R_b)P_b}]}{2(R_a + R_b)} \tag{9}$$

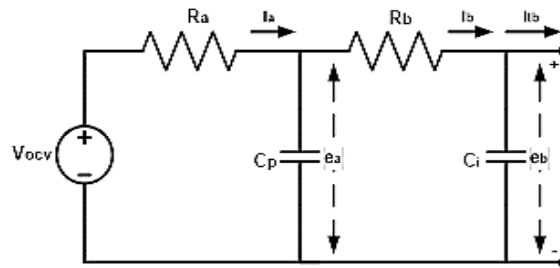


Figure 4. BSU circuit diagram

Table 3. Model specifications for lithium-ion battery

Specification	Value
R_a	0.21 Ω
Initial SOC	90%
Nominal voltage	500 V
Rated Capacity	35.71 h

3. HRGS PROPOSED CONTROL STRATEGY

The different components in Figure 1 are used to regulate the systems that will be discussed later. The purpose of each block control strategy of HRGS connected to the grid is described in detail in the sections below.

3.1. PV Module's boost converter control

Figure 1 depicted the boost converter is connected to the PV section. The boost converter's job is to raise the PV module's input voltage level. The boost converter's input voltage is lower than the output voltage. MPPT generates gate pulses, which are used to operate the boost converter's switch. Because of air

conditions and the Sun's position, the sun's irradiation level varies and always varies from time to time. MPPT employs an improved P&O approach to correctly track maximum power.

3.2. Charging and discharging control strategy for BSU

During day time, the BSU stores the energy generated by PV panels. The stored power is charged until it reaches its full capacity, and then it must be given to the grid during the night. Discharging is the term for this procedure. It will be tough to supply the grid if PV generation is not sufficient owing to poor weather conditions. However, the BSU's stored energy can manage power to feed the grid for a short period of time. At the same time, AU must be turned on right away in order to meet the grid's power needs. This sort of power management, which includes BSU and AU, must be appropriately coordinated with the grid. The BSU is connected to the common DC bus via a DC/DC bi-directional converter in this system. The converter circulates the power in both ways. Using the MPPT algorithm, this new power management, which includes PV cells, may be done during the day. The control approach for the bi-directional converter is depicted in Figure 5. When the V_{dc} output is compared to the V_{dc} , it is passed to the PI controller. The output of the PI controller is once again coupled with I_{batt} , and the complete output is delivered to PWM. The circuit diagram of a BSU-connected buck-boost converter is shown in Figure 5. The control system's T1 and T2 are used to charge and discharge the BSU.

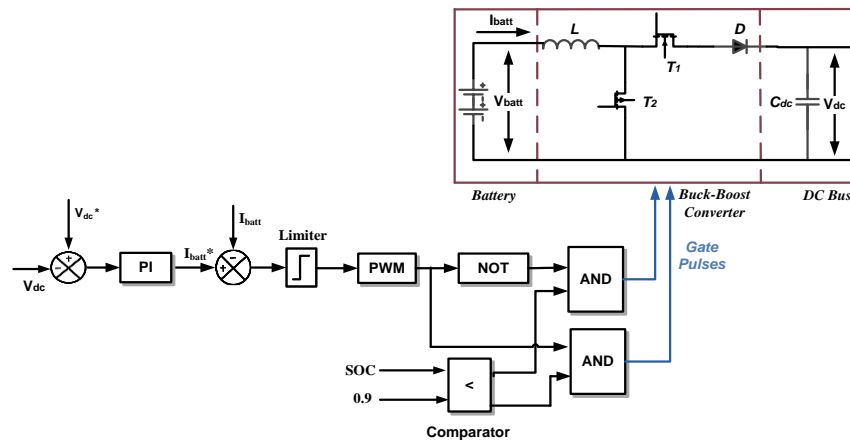


Figure 5. Control circuit for a BSU-connected buck-boost converter

3.3. AU control schemes

In this project, an AU is employed, and its purpose is to give electricity during emergency situations. As a result, AU serves as a backup power source. If the PV system's power generation is insufficient, and the BSU is unable to give the store energy to the grid, the AU can produce electricity and meet the microgrid's requirements. When the PV module is not sufficient to charge the battery, the additional power is used to charge the BSU. Figure 6 depicts the AU connected to boost converter control circuit.

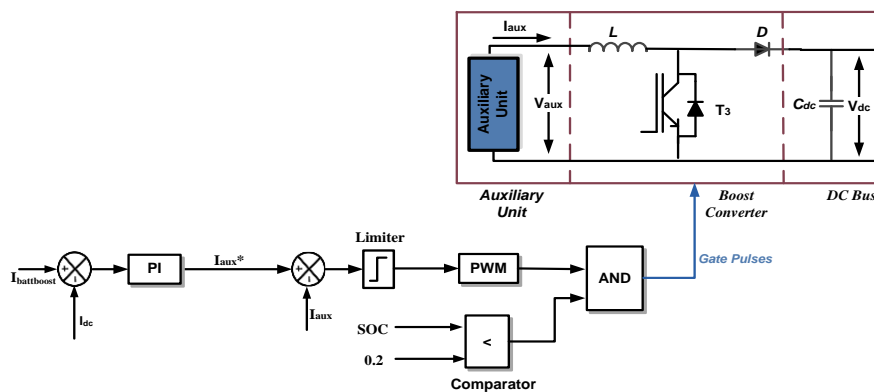


Figure 6. AU connected to the boost converter control circuit

3.4. Control strategy for VSCC

As revealed from Figure 1, the HRGS is coupled to the microgrid via the 3ϕ VSI. The HRGS voltage is synchronized with the grid voltage using VSCC. VSCC's circuit diagram is shown in Figure 7. V_a, V_b, V_c or (V_{abc}) and I_a, I_b, I_c or (I_{abc}) of Voltage and current waveforms from three phases are combined into direct and quadrature axes such as v_d, v_q, i_d, i_q respectively using $abc \rightarrow dq$ converter. For controlling purposes, the benefits of converting AC components to DC components are exploited. Regulating DC components is easier than controlling AC components. In the VSCC, the PLL is utilized to calculate the phase angle Θ from the microgrid voltages. Figure 8 shows a schematic diagram of a PLL. This angle Θ is utilized in converting to $abc \rightarrow dq$ and $dq \rightarrow abc$ converters. P_{grid_ref} and Q_{grid_ref} are used as the reference values of the inverter. P_{grid} and Q_{grid} are the active and reactive powers after the transformation of dq reference frame mentioned in (10) and (11) from [1], [38], [39]. The grid voltage is balanced in q-axis reference frame ($v_q = 0$) and i_{d_ref}, i_{q_ref} are obtained by dividing P_{grid_ref} and Q_{grid_ref} with V_d . Then, i_{d_ref} and i_{q_ref} are compared with i_d and i_q respectively. The outputs are fed to the PI controllers to get, V_{d_ref} and V_{q_ref} . The v_{d_i} and v_{q_i} are calculated by using (12) and (13). Then these values are given to the $dq \rightarrow abc$ converter and the output of $dq \rightarrow abc$ is fed to PWM to produces the pulses. Such pulses are fed to inverter as depicted in Figure 8.

$$P_{grid} = \frac{3}{2}(v_d i_d + v_q i_q) \tag{10}$$

$$Q_{grid} = \frac{3}{2}(v_d i_q - v_q i_d) \tag{11}$$

$$v_{d_i} = -v_{d_ref} + \omega L_f i_q + v_d \tag{12}$$

$$v_{q_i} = -v_{q_ref} - \omega L_f i_d \tag{13}$$

The 3ϕ inverter in the synchronous reference frame, output voltages are;

$$\begin{cases} v_{d_inv} = R_f i_d + L_f \frac{di_d}{dt} - \omega L_f i_q + v_d \\ v_{q_inv} = R_f i_q + L_f \frac{di_q}{dt} + \omega L_f i_d + v_q \end{cases} \tag{14}$$

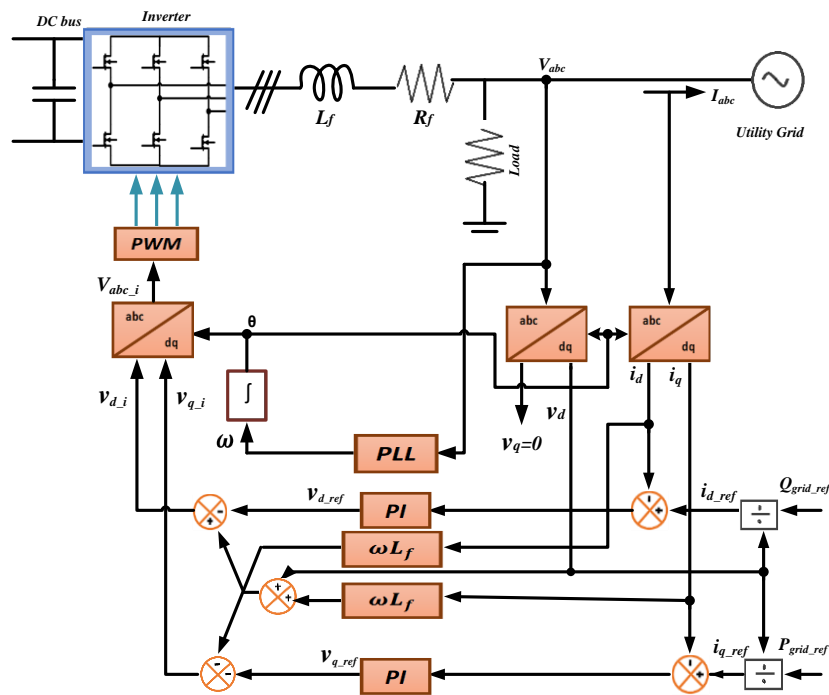


Figure 7. Circuit diagram of VSCC

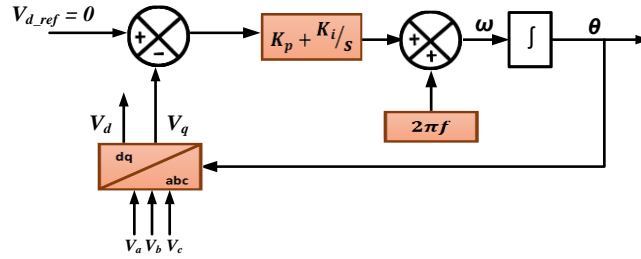


Figure 8. Diagrammatic representation of PLL

3.5. Supervisory control scheme (SCS) of HRGS

Figure 9 depicts the work flow of SCS used in suggested HRGS model. The 2 types of loads are taken here. First, we have considered a nonlinear load (L_1) and second one is of variable load (L_2). When V_{dc} is less than V_{dc}^* , then BSU discharges its power and supply to the load, otherwise it checks the level of SOC. If SOC level is greater than 90% (0.9) then BSU provide the strength to the load. If the SOC range is between $0.2 < SOC < 0.9$, then the load demand is fulfilled by the HRGS supply. If $P_{pv} > P_{Load}$, then P_{pv} fulfills the load requirement (P_{Load}) and it charges the BSU. If $P_{pv} + P_{batt} < P_{Load}$, then L_2 is disconnected and L_1 is continued to supply in that situation the SCS checks the SOC level. If $SOC > 0.2$ then the AU charges the BSU and continued to supply the L_1 demand.

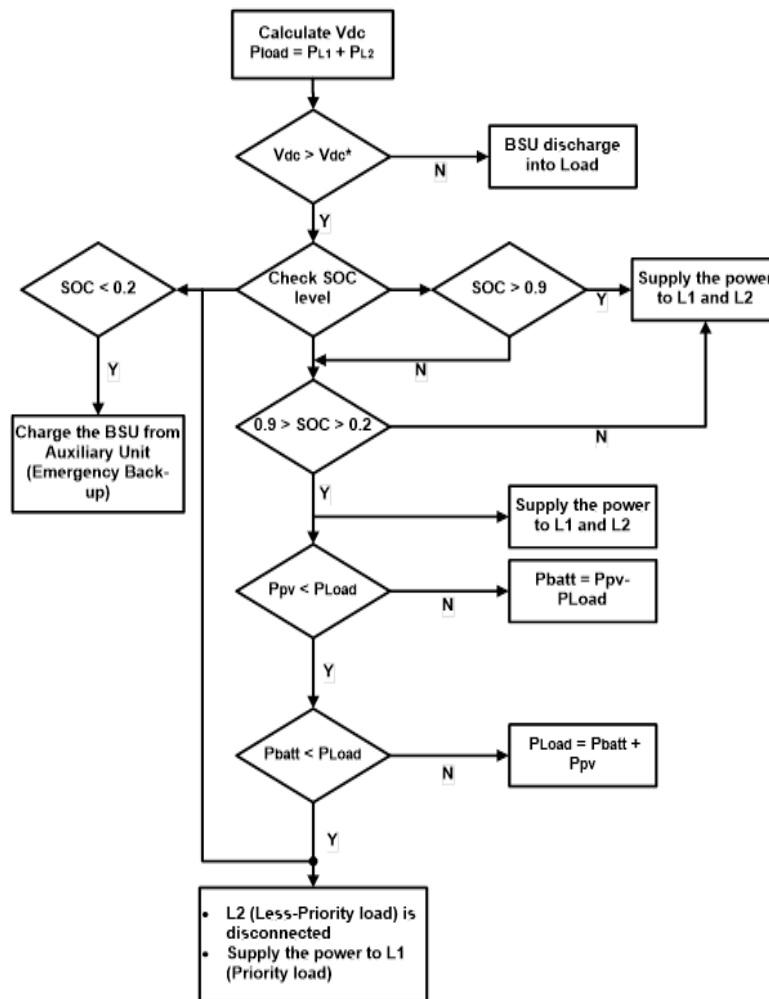


Figure 9. Flowchart of HRGS using SCS

4. RESULTS AND DISCUSSION

The suggested HRGS scheme shown above was created with latest version of the MATLAB/SIMULINK. The HRGS power management model performance and controlling scheme were explored in detail in the following sections. HRGS waveforms have been proven under a variety of grid-connected load conditions. Figure 10 depicts the various irradiation levels of a PV system.

Figure 11 represents the boost converter's power output when interconnected to the PV system, while Figure 12 depicts the load powers gained by various sorts of loads, like as priority load (L1) and less-priority load (L2). The SOC level of the BSU as represented in Figure 13. Figure 11 represents the PV model, power is zero during the time interval 0-to-1.4 seconds, and then grows for the time interval 1.4-to-3 seconds as the radiation level grows, as illustrated in Figure 10.

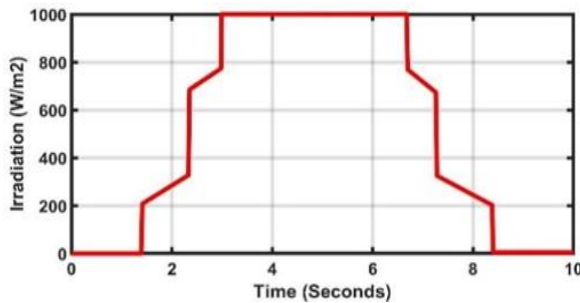


Figure 10. PV system's irradiation level

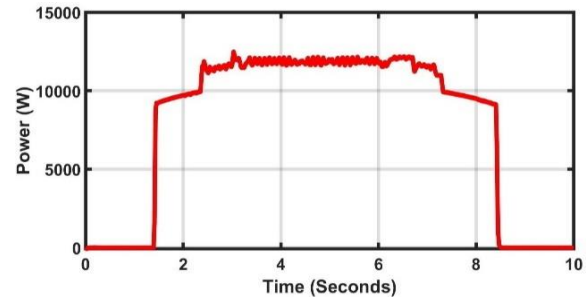


Figure 11. PV module power output (P_{pv})

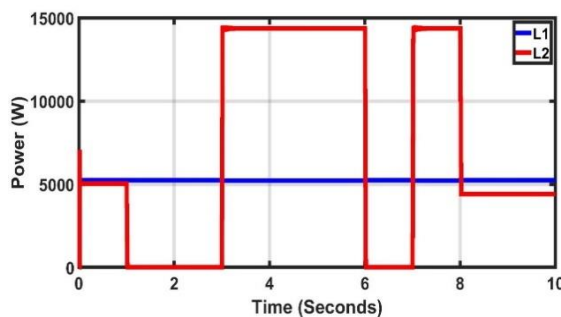


Figure 12. Power consumed by L1 and L2

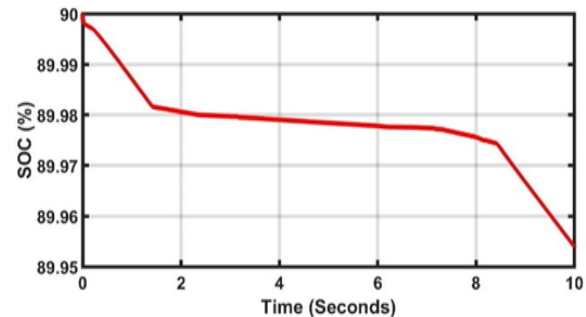


Figure 13. SOC level of the BSU

While a result, SOC level drops fast between 0 and 1.4 seconds as $P_{pv} = 0$ is used to give power to the load. P_{pv} grows in the region of 1.4 to 3 seconds, as shown in Figure 11. As a result, the SOC curve in this time period is less inclined, as seen in Figure 13. The similar event happens between the intervals of 6.7 and 8.4 seconds and 8.4 and 10 seconds. Because $P_{pv} = 0$, the SOC curve is too disposed in this time interval from 8.4-to-10 seconds. Figure 14 shows the Buck-Boost converter's output power over the BSU. The generated power of the bidirectional DC/DC converter linked across the BSU (P_{batt}) is provided to the load as the PV power section zero, as shown in Figure 11 and Figure 14. After that, as PV power grows and becomes capable of serving the demand, it gradually decreases. When the load demand remains in the range of 8.4 to 10 seconds, the P_{batt} increases again as the PV power decreases to zero. In Figure 15, the boost converter output power is coupled across the AU. The AU is ready to move into position to charge the BSU when the SOC level is less than equal to 20% (0.2), as indicated in Figure 9. When PV and BSU power are inadequate to fulfil total load demand, or when both of these powers are insufficient, AU is given to L1, and lower-priority loads are disconnected from the supply. The DC bus voltage of HRGS is shown in Figure 16. The DC bus voltage holds nearly constant during the operation time interval, even when the load demand and HRGS power change, as illustrated in figure. During this time, P_{batt} is increased from 0 to the maximum level, as seen in Figure 14. Figure 17 depicts the voltage waveform of HRGS, whereas Figure 18 discusses the subplot of the voltage waveform of HRGS during the time periods 7.9 and 8.1. The THD of the voltage waveform of HRGS connected to the grid is 0.17 percent, as shown in Figure 19.

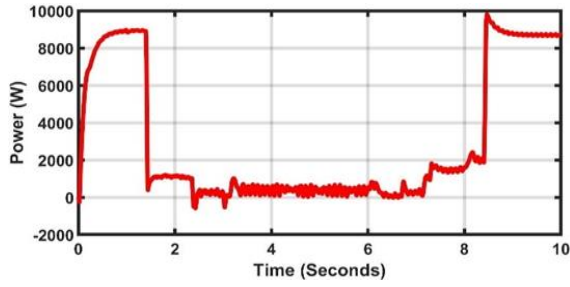


Figure 14. Buck-boost converter output power when connected across the BSU

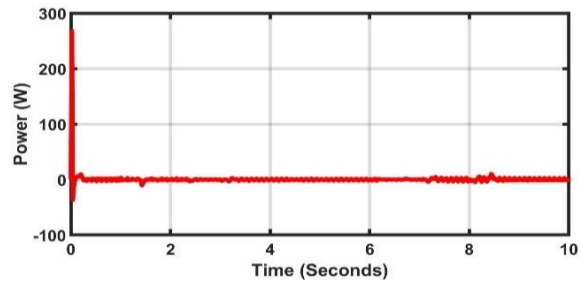


Figure 15. Boost converter output power when connected across the AU

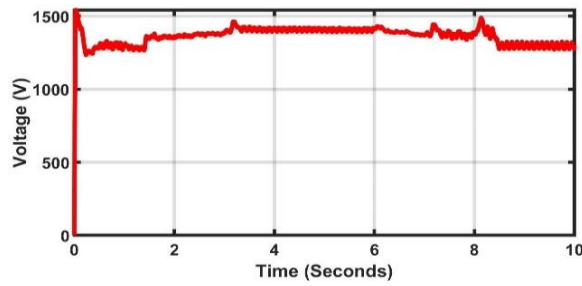


Figure 16. DC bus voltage

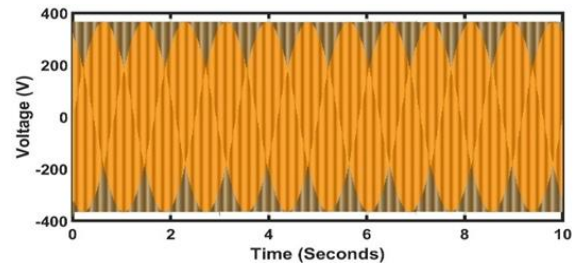


Figure 17. HRGS voltage waveform

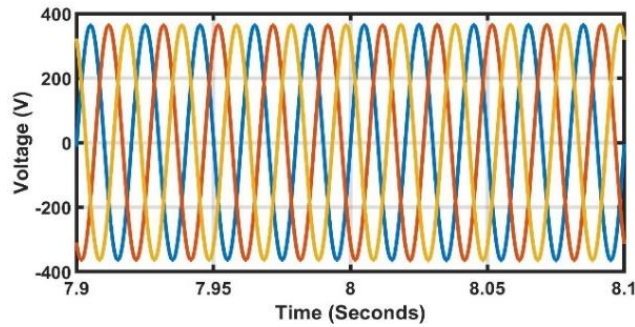


Figure 18. Subplot of HRGS voltage waveform

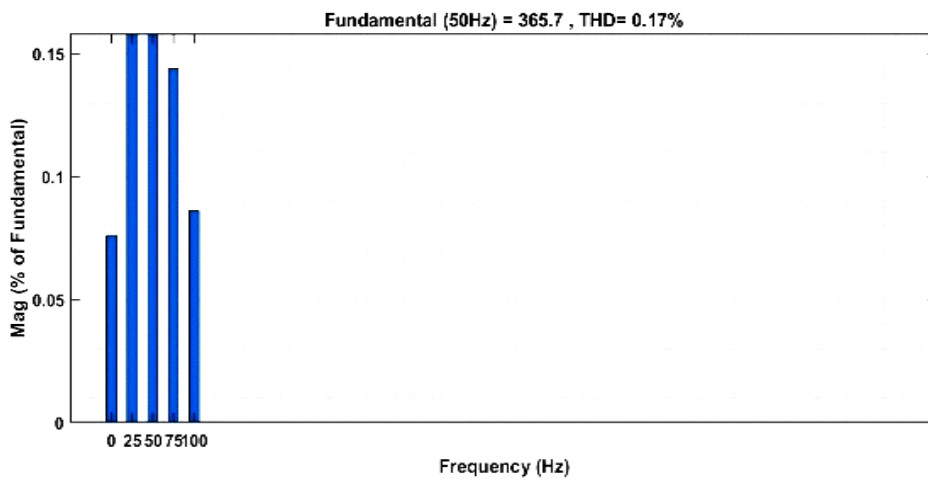


Figure 19. THD study of voltage waveform of HRGS coupled to the grid

Similarly, Figure 20 depicts the current waveform of HRGS, whereas Figure 21 shows the equivalent subplot of the current waveform of HRGS. The present waveform time period continues between 7.9 and 8.1, as shown in Figure 21. In Figure 22, the THD computed from the present signal is 0.14 percent. Figure 23 depicts the voltage waveform of the priority load, whereas Figure 24 depicts the matching subplot of the voltage waveform of the priority load from 7.9 to 8.1. THD is 0.17 percent in the voltage waveform under priority load, as shown in Figure 25.

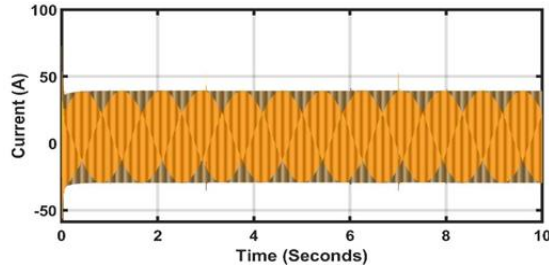


Figure 20. HRGS current waveform

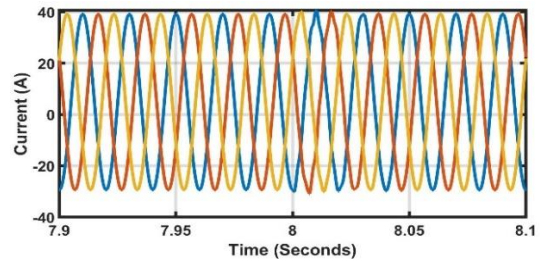


Figure 21. Subplot of HRGS current waveform

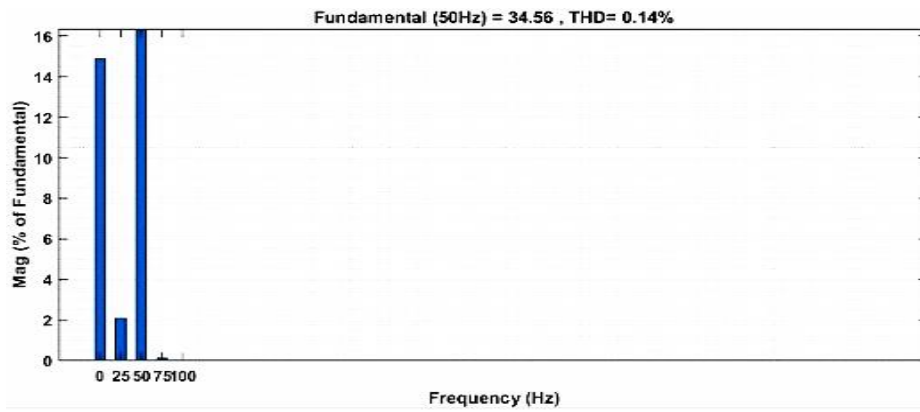


Figure 22. THD study of current waveform of HRGS coupled to the grid

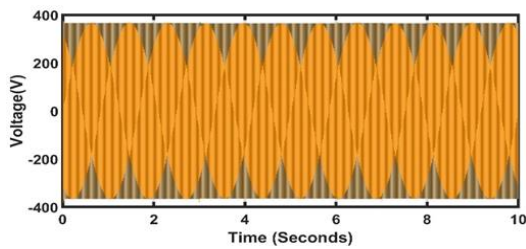


Figure 23. Voltage waveform of L_1

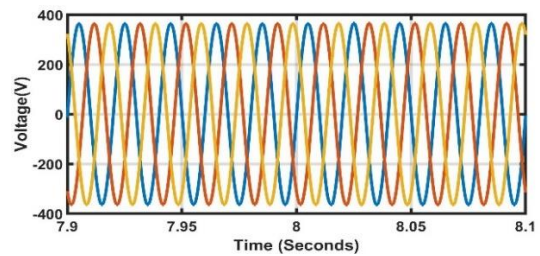


Figure 24. Subplot of L_1 voltage waveform

The priority load current waveform is represented in Figure 26, and the matching subplot of current waveform is depicted in Figure 27 between the time periods 7.9 and 8.1. In this case, the THD is 0.33 percent, as illustrated in Figure 28. The priority load power waveform is shown in Figure 29 and the corresponding subplot of power waveform lies in range of 7.9 to 8.1 as shown in Figure 30. The less-priority load voltage waveform (variable load) is represented in Figure 31 and the corresponding subplot of voltage waveform of low-priority load lies in the range 7.9 to 8.1 shown in Figure 32. The THD found here is 0.42% under less-priority load is shown in Figure 33.

Similarly, current waveform under low priority load is represented in Figure 34, the corresponding subplot of current waveform under low-priority load lies in the range time period 7.9 to 8.1 which is represented in Figure 35. The THD found is 1.00% under low priority load shown in Figure 36. Figure 37 depicts the power waveform of the less-priority load, whereas Figure 38 depicts the equivalent subplot of the power waveform of the less-priority load in the time period 7.9 to 8.1.

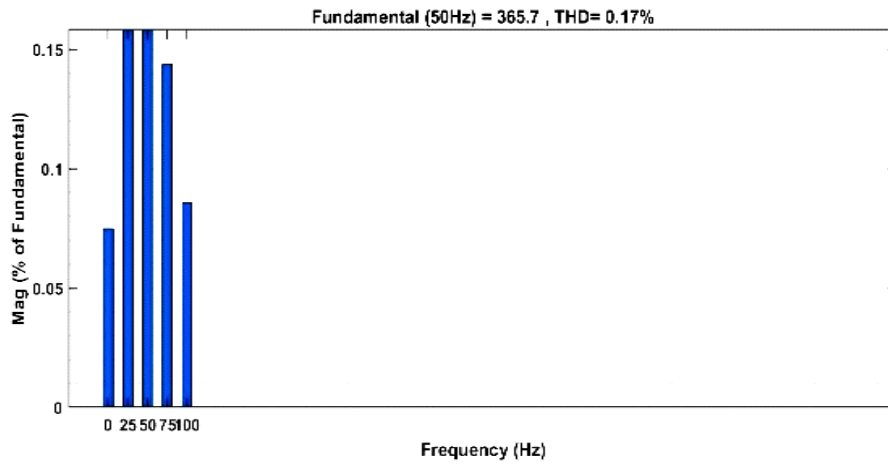


Figure 25. THD study of L_1 voltage waveform

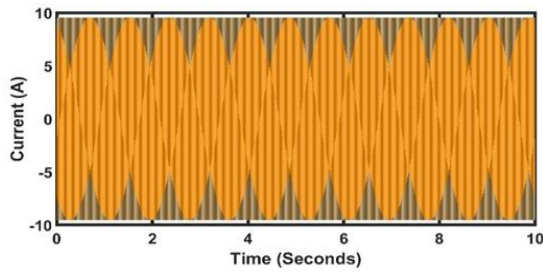


Figure 26. Current waveform of L_1

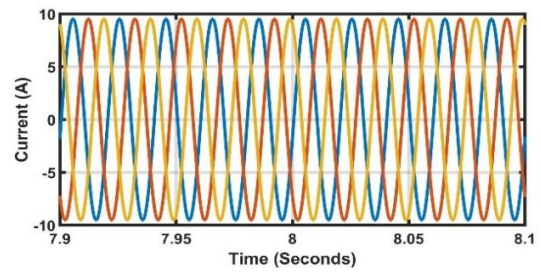


Figure 27. Subplot of L_1 current waveform

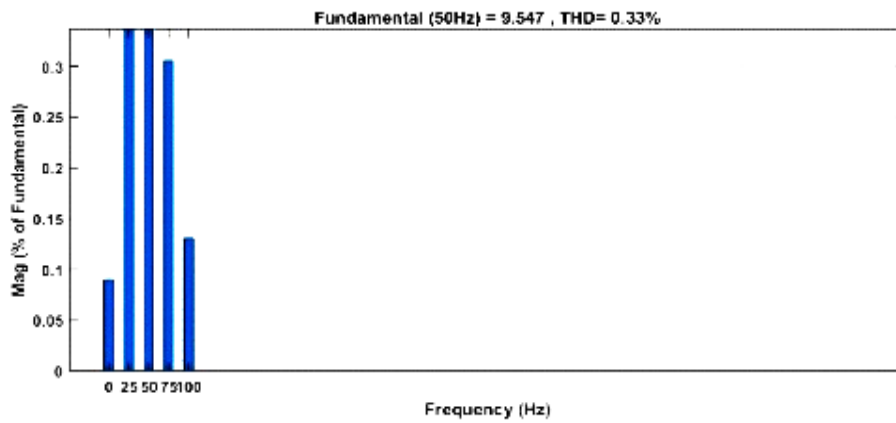


Figure 28. THD analysis of L_1 current waveform

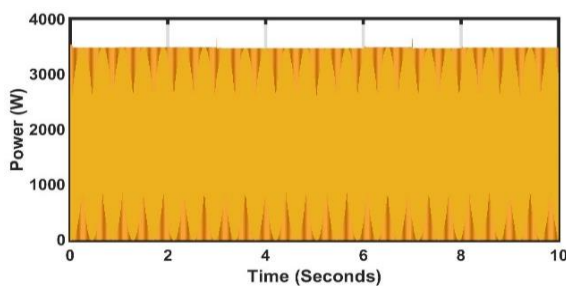


Figure 29. Power waveform of L_1

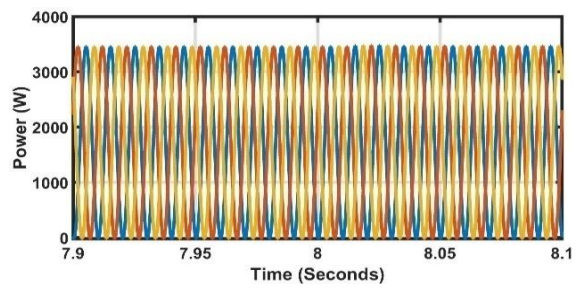


Figure 30. Subplot of L_1 power waveform

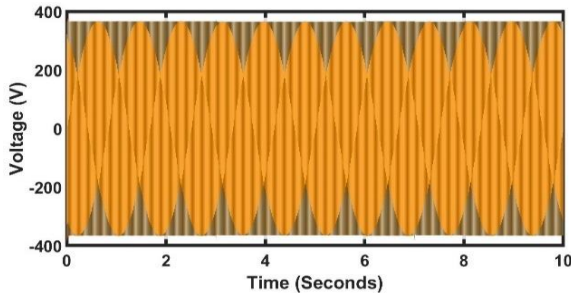


Figure 31. Voltage waveform of L_2

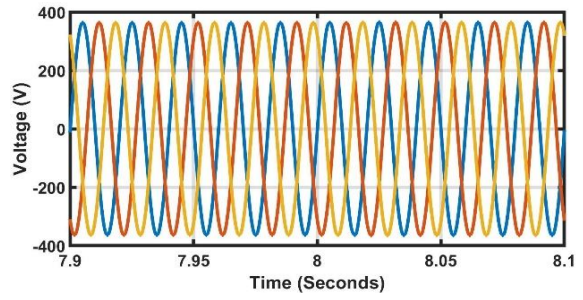


Figure 32. Subplot of L_2 voltage waveform

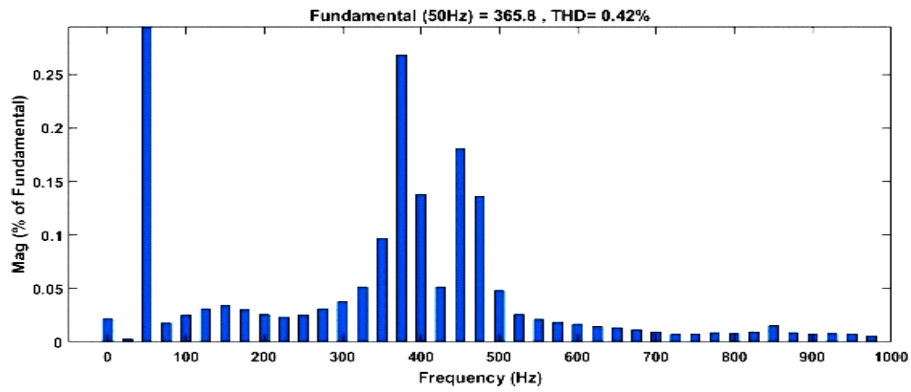


Figure 33. THD analysis of L_2 voltage waveform

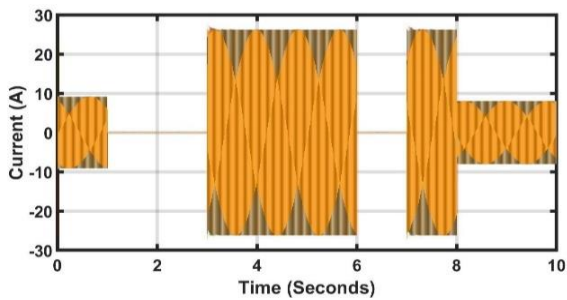


Figure 34. Current waveform of L_2

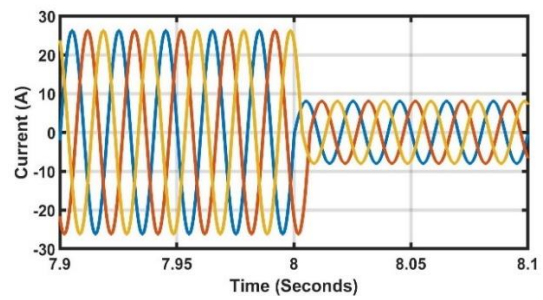


Figure 35. Subplot of L_2 current waveform

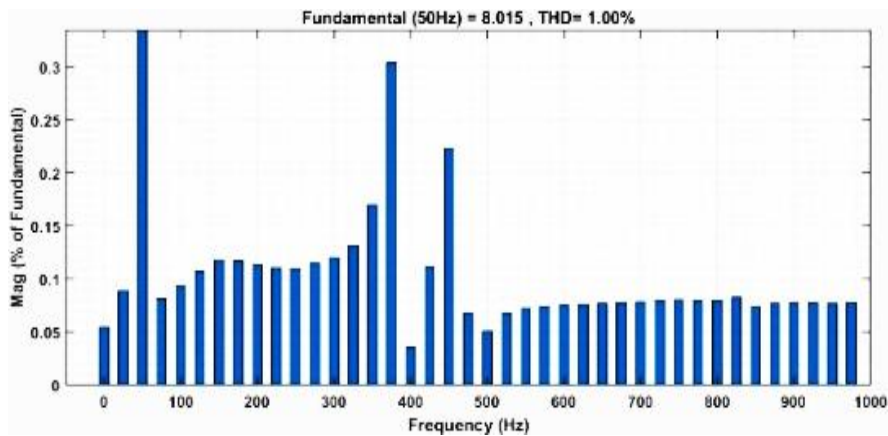
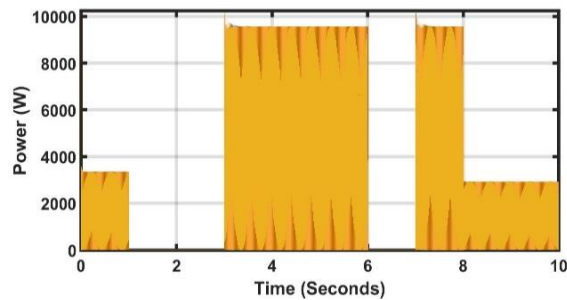
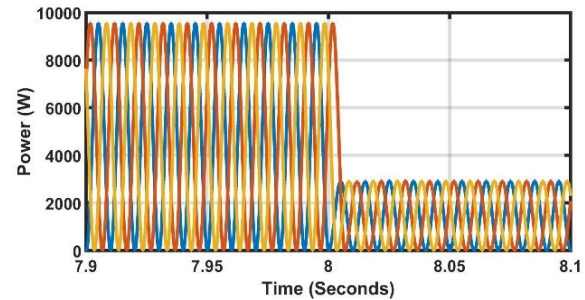


Figure 36. THD analysis of L_2 current waveform

Figure 37. Power waveform of L_2 Figure 38. Subplot of L_2 power waveform

5. CONCLUSION

A novel power management technique as well as the control approach of HRGS coupled to the grid is explored. MATLAB/Simulink 2019 version was used to develop the HRGS model, which comprises of PV, BSU, and AU. At different load conditions based on more and less priority, the performance characteristics of each individual block of the HRGS system, as well as its control method, are shown. When PV power generation is small to charge the battery or the SOC level is below or equal to 20%, however, AU is utilized to charge the BSU on an emergency basis (0.2). To get the most power out of the PV section, a improved P&O approach is employed. In the results section, the Power controlling and managing of the suggested HRGS model that is coupled to the grid have been discussed. PV module and BSU are regarded as HRGS' principal energy sources, with the AU serving as a backup power supply in the event of a power outage. If PV and BSU are not able to fulfill the demand, AU can be used as an emergency power source. However, generation from is relatively costly, yet it is necessary to ensure power supply continuity. A unique SCS is used. The peculiarity of this proposed work is that it aims to improve the performance of power management and control strategies by employing various methods that are tailored to the load demand and restoring supply continuity. The grid voltage is synchronized with the HRGS output voltage using VSCC. Finally, THD analysis is performed for voltage, current, and power signals in order to examine the harmonics level of the waveform and ensure grid smooth functioning.

REFERENCES

- [1] A. Guichi, A. Talha, E. M. Berkouk, and S. Mekhilef, "Energy management and performance evaluation of grid connected PV-battery hybrid system with inherent control scheme," *Sustainable Cities and Society*, vol. 41, pp. 490–504, Aug. 2018, doi: 10.1016/j.scs.2018.05.026.
- [2] U.S. Energy Information Administration, "International energy outlook 2016," vol. 0484, 2016, pp. 1-256.
- [3] F. Birol, "Key world energy statistics," International Energy Agency, 2016, pp. 1-80.
- [4] P. Frankl, "Technology roadmap solar photovoltaic energy," International Energy Agency, 2014, pp. 1-48.
- [5] S. K. Bhuyan, P. K. Hota and B. Panda, "Modeling and simulation of hybrid energy system supplying 3ϕ load and its power quality analysis," *International Journal of Renewable Energy Research*, vol. 8, 2018, pp. 592–603.
- [6] S. K. Bhuyan, P. K. Hota and B. Panda, "Modeling, control and power management strategy of a grid connected hybrid energy system," *International Journal of Electrical and Computer Engineering*, vol. 8, 2018, pp. 1345–1356. doi: 10.11591/ijece.v8i3.pp1345-1356.
- [7] S. Charfi, A. Atieh, and M. Chaabene, "Modeling and cost analysis for different PV/battery/diesel operating options driving a load in Tunisia, Jordan and KSA," *Sustainable Cities and Society*, vol. 25, pp. 49–56, Aug. 2016, doi: 10.1016/j.scs.2016.02.006.
- [8] W. Libo, Z. Zhengming and L. Jianzheng, "A single-stage three-phase grid-connected photovoltaic system with modified MPPT method and reactive power compensation," in *IEEE Transactions on Energy Conversion*, vol. 22, no. 4, pp. 881–886, Dec. 2007, doi: 10.1109/TEC.2007.895461.
- [9] E. Roman, R. Alonso, P. Ibanez, S. Elorduizapatarietxe and D. Goitia, "Intelligent PV module for grid-connected PV systems," in *IEEE Transactions on Industrial Electronics*, vol. 53, no. 4, pp. 1066–1073, June 2006, doi: 10.1109/TIE.2006.878327.
- [10] A. Maleki, and A. Askarzadeh, "Optimal sizing of a PV/wind/diesel system with battery storage for electrification to an off-grid remote region: A case study of Rafsanjan, Iran," *Sustainable Energy Technologies and Assessments*, vol. 7, pp. 147–153, Sep. 2014, doi: 10.1016/j.seta.2014.04.005.
- [11] G. Notton, V. Lazarov, and L. Stoyanov, "Optimal sizing of a grid-connected PV system for various PV module technologies and inclinations, inverter efficiency characteristics and locations," *Renewable Energy*, vol. 35, no. 2, pp. 541–554, Feb. 2010, doi: 10.1016/j.renene.2009.07.013.
- [12] B. Yang, W. Li, Y. Zhao and X. He, "Design and analysis of a grid-connected photovoltaic power system," in *IEEE Transactions on Power Electronics*, vol. 25, no. 4, pp. 992–1000, April 2010, doi: 10.1109/TPEL.2009.2036432.
- [13] M. Shahparasti, A. Sadeghi Larijani, A. Fatemi, A. Yazdian Varjani and M. Mohammadian, "Quasi Z-source inverter for photovoltaic system connected to single phase AC grid," *2010 1st Power Electronic & Drive Systems & Technologies Conference (PEDSTC)*, 2010, pp. 456–460, doi: 10.1109/PEDSTC.2010.5471773.

- [14] J. Selvaraj and N. A. Rahim, "Multilevel inverter for grid-connected PV system employing digital PI controller," in *IEEE Transactions on Industrial Electronics*, vol. 56, no. 1, pp. 149–158, Jan. 2009, doi: 10.1109/TIE.2008.928116.
- [15] Y. Karimi, H. Oraee, M. S. Golsorkhi and J. M. Guerrero, "Decentralized method for load sharing and power management in a PV/battery hybrid source islanded microgrid," in *IEEE Transactions on Power Electronics*, vol. 32, no. 5, pp. 3525–3535, May 2017, doi: 10.1109/TPEL.2016.2582837.
- [16] S. K. Mishra, S. K. Bhuyan, and P. V. Rathod, "Performance analysis of a hybrid renewable generation system connected to grid in the presence of DVR," *Ain Shams Engineering Journal*, vol. 13, no. 4, pp. 1–17, Jun. 2022, doi: 10.1016/j.asej.2022.101700.
- [17] M. S. Golsorkhi, Q. Shafiee, D. D. -C. Lu and J. M. Guerrero, "A distributed control framework for integrated photovoltaic-battery-based islanded microgrids," in *IEEE Transactions on Smart Grid*, vol. 8, no. 6, pp. 2837–2848, Nov. 2017, doi: 10.1109/TSG.2016.2593030.
- [18] F. Zaouche, D. Rekioua, J.-P. Gaubert, and Z. Mokrani, "Supervision and control strategy for photovoltaic generators with battery storage," *International Journal of Hydrogen Energy*, vol. 42, no. 30, pp. 19536–19555, Jul. 2017, doi: 10.1016/j.ijhydene.2017.06.107.
- [19] M. Kim and S. Bae, "Decentralized control of a scalable photovoltaic (PV)-battery hybrid power system," *Applied Energy*, vol. 188, pp. 444–455, Feb. 2017, doi: 10.1016/j.apenergy.2016.12.037.
- [20] Z. Yi, W. Dong and A. H. Etemadi, "A unified control and power management scheme for PV-battery-based hybrid microgrids for both grid-connected and islanded modes," in *IEEE Transactions on Smart Grid*, vol. 9, no. 6, pp. 5975–5985, Nov. 2018, doi: 10.1109/TSG.2017.2700332.
- [21] A. S. O. Ogunjuigbe, C. G. Monyei, and T. R. Ayodele, "Price based demand side management: A persuasive smart energy management system for low/medium income earners," *Sustainable Cities and Society*, vol. 17, pp. 80–94, Sep. 2015, doi: 10.1016/j.scs.2015.04.004.
- [22] P. Rathod, S. K. Mishra, S. K. Bhuyan, "Renewable energy generation system connected to micro grid & analysis of energy management," *International Journal of Power Electronics and Drive System (IJPEDS)*, vol. 11, no. 3, Sep 2020, doi: 10.11591/ijpeds.v13.i1.pp470-479.
- [23] F. A. Mohamed and H. N. Koivo, "MicroGrid online management and balancing using multiobjective optimization," *2007 IEEE Lausanne Power Tech*, 2007, pp. 639–644, doi: 10.1109/PCT.2007.4538391.
- [24] N. J. Williams, P. Jaramillo and J. Taneja, "PV-array sizing in hybrid diesel/PV/battery microgrids under uncertainty," *2016 IEEE PES PowerAfrica*, 2016, pp. 189–193, doi: 10.1109/PowerAfrica.2016.7556598.
- [25] R. Hosseinalizadeh, H. Shakouri G, M. Amalnick, and P. Taghipour, "Economic sizing of a hybrid (PV–WT–FC) renewable energy system (HRES) for stand-alone usages by an optimization-simulation model: Case study of Iran," *Renewable and Sustainable Energy Reviews*, vol. 54, pp. 139–150, Feb. 2016, doi: 10.1016/j.rser.2015.09.046.
- [26] S. B. Utomo, I. Setiawan, B. Fajar, S. H. Winoto, and A. Marwanto "Optimizing of the installed capacity of hybrid renewable energy with a modified MPPT model," *International Journal of Electrical and Computer Engineering (IJECE)*, vol. 12, no. 1, 2022, pp. 73–81, doi: 10.11591/ijece.v12i1.pp73-81.
- [27] M. J. Khan, A. K. Yadav, and L. Mathew, "Techno economic feasibility analysis of different combinations of PV-Wind-Diesel-Battery hybrid system for telecommunication applications in different cities of Punjab, India," *Renewable and Sustainable Energy Reviews*, vol. 76, pp. 577–607, Sep. 2017, doi: 10.1016/j.rser.2017.03.076.
- [28] N. Nitta, F. Wu, J. T. Lee, and G. Yushin, "Li-ion battery materials: present and future," *Materials Today*, vol. 18, no. 5, pp. 252–264, 2015, doi: 10.1016/j.mattod.2014.10.040.
- [29] M. Ouremchi, S. El Mouzouade, K. El Khadiri, A. Tahiri, and H. Qjidaa "Integrated energy management converter based on maximum power point tracking for photovoltaicsolar system," *International Journal of Electrical and Computer Engineering (IJECE)*, vol. 12, no. 2, 2022, pp. 1211–1222, doi: 10.11591/ijece.v12i2.pp1211-1222.
- [30] M. G. Villaiva, J. R. Gazoli and E. R. Filho, "Modeling and circuit-based simulation of photovoltaic arrays," *2009 Brazilian Power Electronics Conference*, 2009, pp. 1244–1254, doi: 10.1109/COBEP.2009.5347680.
- [31] A. Laudani, F. Riganti Fulginei, and A. Salvini, "Identification of the one-diode model for photovoltaic modules from datasheet values," *Solar Energy*, vol. 108, pp. 432–446, Oct. 2014, doi: 10.1016/j.solener.2014.07.024.
- [32] S. K. Bhuyan, P. K. Hota, and B. Panda, "Power quality analysis of a grid-connected solar/wind/hydrogen energy hybrid generation system," *International Journal of Power Electronics and Drive Systems (IJPEDS)*, vol. 9, no. 1, p. 377, Mar. 2018, doi: 10.11591/ijpeds.v9.i1.pp377-389.
- [33] A. Belkaid, I. Colak, and K. Kayisli, "Implementation of a modified P&O-MPPT algorithm adapted for varying solar radiation conditions," *Electrical Engineering*, vol. 99, no. 3, pp. 839–846, Oct. 2016, doi: 10.1007/s00202-016-0457-3.
- [34] I. Yahyaoui, M. Chaabene, and F. Tadeo, "Evaluation of maximum power point tracking algorithm for off-grid photovoltaic pumping," *Sustainable Cities and Society*, vol. 25, pp. 65–73, Aug. 2016, doi: 10.1016/j.scs.2015.11.005.
- [35] R. Alik and A. Jusoh, "Modified perturb and observe (P&O) with checking algorithm under various solar irradiation," *Solar Energy*, vol. 148, pp. 128–139, May 2017, doi: 10.1016/j.solener.2017.03.064.
- [36] A. Gupta, P. Kumar, R. K. Pachauri and Y. K. Chauhan, "Performance analysis of neural network and fuzzy logic based MPPT techniques for solar PV systems," *2014 6th IEEE Power India International Conference (PIICON)*, 2014, pp. 1–6, doi: 10.1109/POWERI.2014.7117722.
- [37] A. Hajizadeh and M. A. Golkar, "Intelligent power management strategy of hybrid distributed generation system," *International Journal of Electrical Power & Energy Systems*, vol. 29, no. 10, pp. 783–795, Dec. 2007, doi: 10.1016/j.ijepes.2007.06.025.
- [38] R. Kadri, J. -P. Gaubert and G. Champenois, "An improved maximum power point tracking for photovoltaic grid-connected inverter based on voltage-oriented control," in *IEEE Transactions on Industrial Electronics*, vol. 58, no. 1, pp. 66–75, Jan. 2011, doi: 10.1109/TIE.2010.2044733.
- [39] Y. Errami, M. Maaroufi and M. Ouassaid, "Modelling and control strategy of PMSG based variable speed wind energy conversion system," *2011 International Conference on Multimedia Computing and Systems*, 2011, pp. 1–6, doi: 10.1109/ICMCS.2011.5945736.

BIOGRAPHIES OF AUTHORS

Pranita Rathod     has graduated & post graduated in Electrical and power Engineering from Government College of Engineering, Amravati, India in 2012 and 2017 respectively. Her research interest includes renewable generation systems, micro grid and power system analysis. She can be contacted at email: pranita.rathod@ghru.edu.in.



Sujit Kumar Bhuyan     has graduated and post graduated in Electrical Engineering in 2007 and 2012 respectively and completed his Ph.D. in 2019 from KIIT University, Bhubaneswar, India. Currently, he is working as a head of Resource Assessment and Asset Analysis (RAAA) in Manikaran Analytics Limited, Delhi, India. His research interests include Renewable Energy Generation Systems, Power Electronics Converters and Inverters, Machine Learning, Data Science and soft computing. He is also the reviewer of Elsevier, IEEE Access and Springer. He can be contacted at email: sujit.kumar84@gmail.com.



Sanjoy Kumar Mishra     has received the Ph.D. in Electrical Engineering from KIIT University, Bhubaneswar, India. Master in Engineering and Bachelor in 2003 & 1995 respectively. Currently, he is working as Associate Professor in Electrical Engineering from G. H. Rasoni University, Amravati, India. His area of interest includes soft computing tools applying in power system stability, signal processing algorithm in power system protection and hybrid energy and micro grid. He is also the reviewer of Elsevier, IEEE Access and IEEE system Journal. He can be contacted at email: sanjay29y@gmail.com.